

Fragmentation Trees Reloaded

Kai Dührkop and Sebastian Böcker

Chair for Bioinformatics, Friedrich-Schiller-University, Jena, Germany,
{kai.duehrkop, sebastian.boecker}@uni-jena.de

Abstract. Metabolites, small molecules that are involved in cellular reactions, provide a direct functional signature of cellular state. Untargeted metabolomics experiments usually relies on tandem mass spectrometry to identify the thousands of compounds in a biological sample. Today, the vast majority of metabolites remain unknown. Fragmentation trees have become a powerful tool for the interpretation of tandem mass spectrometry data of small molecules. These trees are found by combinatorial optimization, and aim at explaining the experimental data via fragmentation cascades. To obtain biochemically meaningful results requires an elaborate optimization function.

We present a new scoring for computing fragmentation trees, transforming the combinatorial optimization into a maximum a posteriori estimator. We demonstrate the superiority of the new scoring for two tasks: Both for the de novo identification of molecular formulas of unknown compounds, and for searching a database for structurally similar compounds, our methods performs significantly better than the previous scoring, as well as other methods for this task. Our method can expedite the workflow for untargeted metabolomics, allowing researchers to investigate unknowns using automated computational methods.

1 Introduction

Metabolites, small molecules that are involved in cellular reactions, provide a direct functional signature of cellular state complementary to the information obtained from genes, transcripts and proteins. Research in the field of metabolomics can give insight for biomarkers detection, cellular biochemistry, and disease pathogenesis [2, 19, 29, 32]; whereas natural product research screens metabolites for novel drug leads [6, 13]. With advances in mass spectrometry instrumentation, it is now possible to detect thousands of metabolites simultaneously from a biological sample.

Metabolomics experiments often use a targeted approach in which only a specified list of metabolites is measured. This setup allows profiling these metabolites with high speed, minimal effort and limited resources over a large number of samples. Unfortunately, the vast majority of metabolites remain unknown [2, 19], and this is particularly the case for non-model organisms and secondary metabolites. The structural diversity of metabolites is extraordinarily large; in almost all cases, we cannot deduce the structure of metabolites from genome sequences. To this end, untargeted metabolomics comprehensively compares the intensities of thousands of metabolite peaks between two or more samples. Here, a major challenge is to determine the identities of those peaks that exhibit some fold change. For this, tandem mass spectrometry data of the compounds is usually searched against a spectral library such as Massbank [11] or the Human Metabolome Database [30].

Only few computational methods exist that target compounds not contained in a spectral library [12, 25]: In particular, certain methods try to replace spectral libraries by the more comprehensive molecular structure databases for searching [1, 9, 10, 31]. But these methods must fail for compounds not present in a structure database. Methods for predicting the molecular formula of an unknown compound usually require data beyond tandem mass spectra [3, 16, 20, 24]. Fragmentation trees (FTs) were introduced to fill this gap [5], and were later shown to contain viable structural information about the unknown compound [22]. FT computation does not require any (spectral, structural, or other) databases.

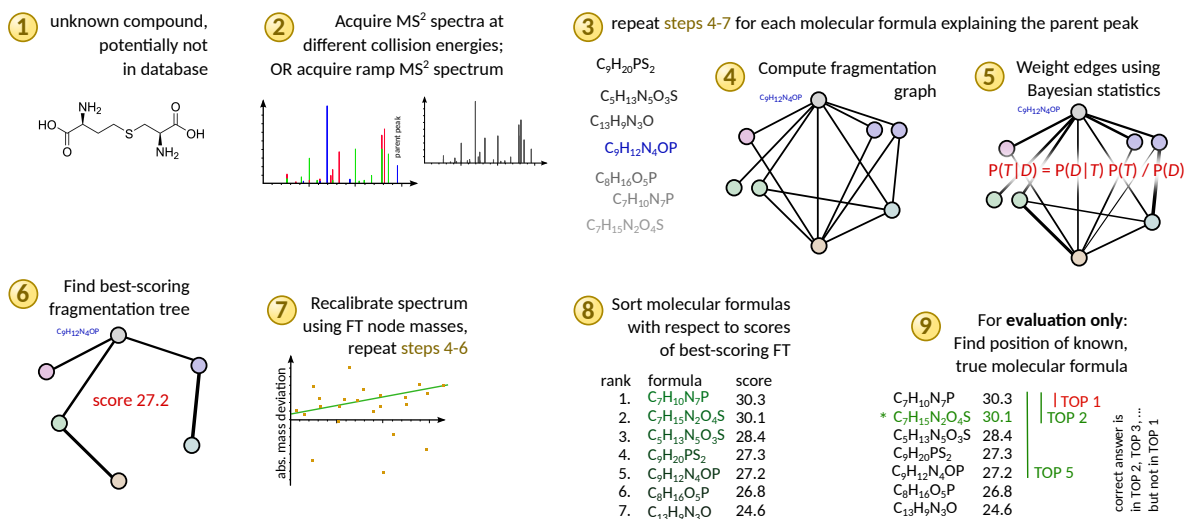


Fig. 1. Workflow of our method for computing FT to predict the correct molecular formula of the ion peak of MS/MS spectra.

In this paper, we report a systematic approach for choosing the fragmentation tree that best explains the observed data, based on Bayesian analysis and a maximum a posteriori estimation. As conjectured in [22] this results in a strong increase in FT quality, as we evaluate using two derived measures: Both for the de novo identification of molecular formulas of unknown compounds, and for searching a database for chemically similar compounds, the new FTs perform significantly better than state-of-the-art methods.

Our method will be made available on our website¹ as new version of the SIRIUS framework for MS and MS/MS analysis. See Fig. 1 for a schematic workflow of our method.

2 Fragmentation Trees

First, we will formally introduce fragmentation trees, allowing us to interpret fragmentation tree computation as a maximum a posteriori estimation in the next section. Our *data* $\mathcal{D} = (\mathcal{M}, I)$ is a measured fragmentation spectrum with peak masses $\mathcal{M} = \{m_1, \dots, m_L\}$ and peak intensities $I : \mathcal{M} \rightarrow \mathbb{R}_{>0}$. Masses are not measured with arbitrary precision: To decide whether some theoretical molecular formula may coincide with some measured peak, we use a relative mass accuracy parameter MA provided by the user. Fragmentation spectra are relatively sparse: For any interval of 1 Da in the spectrum, there is at most a few peaks present. On the other hand, we demand that the mass accuracy of the measurement is high, say, 20 ppm or better. To this end, almost all theoretical molecular formula can explain *at most one* peak in the measured spectrum.

A *fragmentation tree* (FT) $\mathcal{T} = (V, E)$ consists of a set of nodes V which are molecular formulas over some alphabet of elements, and directed edges (arcs) connecting these nodes. All edges are directed away from the root of the tree, and every node can be reached from the root via a unique series of edges. In small compound fragmentation, many fragments result from fragmentation cascades, that is, series of subsequent fragmentation events; these cascades are modeled by the tree structure of the FT. Nodes of the FT are molecular formulas of the unfragmented ion and its fragments; edges correspond to losses. For any FT, each molecular formula can appear at most once

¹ <http://bio.informatik.uni-jena.de/software/>

as a node of the tree. For an edge $(u, v) \in E$, $u - v$ is the molecular formula of the corresponding loss; we demand that $u \geq v$ holds (for each component) and, hence, $u - v \geq 0$. Let $\mu(f)$ denote the theoretical mass of the molecular formula f (either fragment or loss). This will usually be the mass of the lightest naturally occurring isotope of an element, such as $\mu(\text{H}) = 1.007825$.

For a given FT, we can simulate a fragmentation spectrum (without intensities), simply using the masses of all nodes' molecular formulas. For the inverse direction, a FT is supported by a fragmentation spectrum of a (usually unknown) compound if, for every node of the tree, we find a peak in the spectrum such that the mass difference between the molecular formula of the node and the peak mass is below some user-defined threshold. Not all peaks of the fragmentation spectrum have to be explained by the tree, as we also have to consider noise peaks in the spectrum. We demand that every node of the FT explains a *unique* peak in the spectrum: no two nodes of the tree may correspond to the same peak. Allowing more than one node to explain a peak, would violate the vast majority of observations: In theory, it is possible that two fragments of a compound have different structure but very similar mass, so that both fragments would explain the same peak. In practice, this situation is extremely rare and we can safely ignore it.

We now formalize our above considerations. We say that a FT $\mathcal{T} = (V, E)$ is *supported by* the observed data $\mathcal{D} = (\mathcal{M}, I)$ if each node $v \in V$ is assigned a unique peak $m \in \mathcal{M}$ in the fragmentation spectrum that is within the chosen mass accuracy. Furthermore, no two nodes are assigned the same peak. We denote the *natural injective mapping* from the FT nodes to the peaks by $m : V \rightarrow \mathcal{M}$. All peaks in the spectrum not assigned to a node of the FT, are regarded as noise peaks. Our task is to find a FT that “best explains” the observed data, where goodness-of-fit is measured by some scoring function that matches FT and mass spectrum.

This formulation of the problem is not easily accessible by algorithmic means; to this end, Böcker and Rasche [5] gave an alternative formulation which, for additive scorings, is equivalent to the above: For each peak in the fragmentation spectrum, we find all molecular formulas with mass difference sufficiently small. These molecular formulas are the nodes of a directed acyclic graph (DAG) called *fragmentation graph*. Nodes are colored so that all molecular formulas corresponding to the same peak have the same color. Recall that we must use at most one vertex for each color (peak) in our FT. Edges are inserted whenever one molecular formula is a sub-formula of another. Edges are appropriately weighted using some score function. It is straightforward to check that there is a 1-1 correspondence between *colorful subtree*, that use every color in the graph at most once, and FTs supported by the data. We search for a colorful subtree of this graph that has maximum weight. The underlying computational problem has been coined MAXIMUM COLORFUL SUBTREE; unfortunately, this problem is computationally hard [23]. Nevertheless, there exist a number of algorithms (both exact and heuristic) to solve the problem in practice [5, 23]. In this paper, we will not cover any algorithmic details of the problem; we solve our instances using Integer Linear Programming (ILP) as described in [23].

3 Maximum a Posteriori Estimation

Our maximum a posteriori estimate roughly follows the scoring introduced by Böcker and Rasche [5], further refined by Rasche *et al.* [21, 22]. These scorings were motivated by stochastic considerations, but only in an informal way. Here, we will strictly model the problem as a maximum a posteriori estimation, which allows us to make sensible choices for the (hyper)parameters of the method. Bayesian Statistics tell us that

$$\mathbb{P}(\mathcal{T}_j | \mathcal{D}) = \frac{\mathbb{P}(\mathcal{D} | \mathcal{T}_j) \cdot \mathbb{P}(\mathcal{T}_j)}{\mathbb{P}(\mathcal{D})} = \frac{\mathbb{P}(\mathcal{D} | \mathcal{T}_j) \cdot \mathbb{P}(\mathcal{T}_j)}{\sum_i \mathbb{P}(\mathcal{D} | \mathcal{T}_i) \mathbb{P}(\mathcal{T}_i)}, \quad (1)$$

where \mathcal{D} is the data (the measured spectrum) and \mathcal{T}_j are the models (the candidate FTs). We want to maximize the *posterior probability* $\mathbb{P}(\mathcal{T}_j|\mathcal{D})$ which is equivalent to maximizing $\mathbb{P}(\mathcal{D}|\mathcal{T}) \cdot \mathbb{P}(\mathcal{T})$ over all possible models \mathcal{T} . Here, $\mathbb{P}(\mathcal{D}|\mathcal{T})$ is the probability of the data given the model \mathcal{T} , and $\mathbb{P}(\mathcal{T})$ is the *prior probability* of model \mathcal{T} , based on prior information that we have about FTs without considering the actual data \mathcal{D} . We have considerable background information about the prior probability of any given FT: For example, smaller losses are usually more frequent than larger losses, and certain losses such as H₂O or CO turn up very frequently.

We stressed repeatedly that we are interested in those FTs only that are supported by the data. To this end, we demand $\mathbb{P}(\mathcal{D}|\mathcal{T}) = 0$ and, hence, $\mathbb{P}(\mathcal{T}|\mathcal{D}) = 0$ for any tree \mathcal{T} that is *not supported by the data* \mathcal{D} . In the following, we assume that each considered FT is supported by the data.

We now introduce computations for prior probability and likelihood of the tree. Due to space constraints, we defer all details to the long version of this paper.

3.1 Prior Probability of the Tree

We first concentrate on the prior $\mathbb{P}(\mathcal{T})$. We will not demand that priors sum to one but only that the sum $\sum_i \mathbb{P}(\mathcal{T}_i) \mathbb{P}(\mathcal{D}|\mathcal{T}_i)$ converges, what is sufficient for optimizing $\mathbb{P}(\mathcal{T}) \cdot \mathbb{P}(\mathcal{D}|\mathcal{T})$. But this is obviously true: The number of models \mathcal{T}_i we are considering is finite, as we are only consider trees supported by the data. We assume that, for all trees of constant size, prior probabilities of the nodes and edges of \mathcal{T} are independent so that

$$\mathbb{P}(\mathcal{T}) = \mathbb{P}(\text{size } |E| \text{ of the tree}) \cdot \prod_{v \in V} \mathbb{P}(v) \cdot \prod_{e \in E} \mathbb{P}(e).$$

Here, $\mathbb{P}(v)$ is the prior probability to see a particular *fragment* in a FT, and $\mathbb{P}(e)$ is the prior probability to see a particular *loss* in a FT. The independence assumption is obviously violated in reality, but allows us to come up with simple yet meaningful priors. We can simplify this equation, noting that every node of the tree except the root has exactly one incoming edge. For molecular formulas u, v let $P_{\text{edge}}(u, v)$ be the prior that fragment v and loss $u - v$ are simultaneously seen in the tree, and let $P_{\text{root}}(u)$ be the prior that the tree is rooted with molecular formula u . Then,

$$\mathbb{P}(\mathcal{T}) \propto \mathbb{P}(\text{size } |E| \text{ of the tree}) \cdot P_{\text{root}}(r) \cdot \prod_{(u,v) \in E} P_{\text{edge}}(u, v) \quad (2)$$

where r is the root of \mathcal{T} .

Prior of the Root. We use the following uninformative prior to filter out structurally impossible molecular formulas: For each compound, the sum of valences has to be greater than or equal to twice the number of atoms minus one [26]. This corresponds to a non-negative ring double bond equivalent (RDBE) value. In addition, we use five informative priors: First, assume that the compound is not a radical, then the sum of valences is even [26]. If the compound ion is protonated, then the sum of valences of the ion is odd. As both intrinsically charged molecules and free radicals are comparatively rare, we use prior 0.1 for molecular formulas with even sum of valences, and 1 for all others. Second, the ratio between hetero atoms and carbon atoms is usually relatively small for biomolecules [15]. We find that this ratio becomes even more informative if we also exclude oxygen from the hetero atoms. We model the ‘‘hetero minus oxygen to carbon ratio’’ (HMOTCR) using a uniform prior for small ratios, and a Pareto distribution for larger ratios. Third, for the ring double bond equivalent (RDBE), we observed that the value $\text{RDBE}/m^{2/3}$ is roughly normal distributed, where m is the mass of the compound. We use the density of the normal distribution as the prior. The last two priors penalize molecular formulas containing rare elements as well as formulas containing phosphor

atoms without oxygen or sulfur atoms (as 99% of the compounds in KEGG that contain phosphor also contain oxygen or sulfur). The root prior $P_{\text{root}}(r)$ is the product of these five priors. We stress that informative priors never discard any molecular formulas but rather, decrease the scores of these formulas. The root prior becomes less important as more peaks are contained in the spectrum (and nodes in the tree). But for compounds that do not fragment very well the root prior may help to identify the correct molecular formula.

Priors of Edges. The prior probability $P_{\text{edge}}(u, v)$ of an edge $e = (u, v)$ is estimated from different factors, namely prior knowledge about implausible (and radical) losses, the mass of the loss, common losses, as well as common fragments. We first penalize *implausible losses* of an edge (u, v) using a prior $P_{\text{loss-impl}}(u, v)$ on the loss $u - v$. This is a small list of losses that repeatedly turned up during our combinatorial optimization, but that were rejected in the expert evaluation in [22]. In particular, we penalize losses that contain only nitrogen or only carbon; radical losses with certain exceptions; and few losses from a list of losses generated by expert knowledge. Since these are losses that we *do not want to see*, there appears to be no sensible way to learn such implausible losses from the data. Instead, we have to rely on expert knowledge and evaluation of FTs computed by the method, to collect this list. Also, priors for such implausible losses were chosen *ad hoc* as there appears to be no sensible way of learning such penalties from the data.

Regarding the mass of a loss, we assume that large losses are less likely than small losses. Unfortunately, there is only a very small number of annotated FTs available in the literature, and these are usually measured on different instruments (and instrument types) using different experimental setup and, hence, are mostly incomparable. To this end, we chose to estimate the loss mass distribution using FTs determined by our method. Different from [5, 21, 22] we do not penalize the relative size of the mass but rather the mass itself, as this allows for a more stringent incorporation of common losses. Combinatorics dictates that there exists only a small number of losses below, say, 30 Da. Besides certain common losses, this implies that the number of small losses is also small, but increases rapidly until some maximum is reached. Beyond this mass, we find that the probability to observe a loss drops rapidly in the beginning, but stays significantly above zero even for large masses. To model these observations, we use a log-normal distribution as a classical example of a long-tailed distribution.

Some losses turn up more often than we would expect from the loss mass distribution. In [5] a expert-curated list of common losses was introduced, and this list was further refined in [21, 22]. Such hand-curated lists can be incomplete and, worse, prior probabilities have to be chosen *ad hoc*. We chose to learn common losses and their prior probabilities from our training data.

Similar to the root, we want to penalize molecular formulas with extreme "hetero minus oxygen to carbon ratio" (HMOTCR) and RDBE value of a fragment. As proposed in [5] we do not penalize a child if we have already penalized the parent, as both HMOTCR and RDBE values are hereditary. We set the prior to be the minimum value of one and the ratio of the priors of child and parent.

For a FT to be informative, it is useful that the FT includes fragments of small masses, even if the corresponding peaks have small intensities and, possibly as a result, larger mass deviations. The molecular formula identification of peaks with small masses is easier due to fewer possible explanations. Therefore, we add a prior that rewards fragments with small masses.

Finally, we noticed that certain fragments turn up repeatedly in FTs. The explanation for this observation is simple and is known to MS experts for decades: Certain groups such as C_6H_4 (benzyne) or $\text{C}_4\text{H}_7\text{N}$ (pyrroline) can be cleaved off as ions, leading to characteristic peaks in the mass spectra. But giving priors for both common losses *and* common fragments, clearly violates the independence assumption: If we know the molecular formulas of a fragment and one of its losses, then this also tells us the molecular formula of the child fragment. To this end, we chose a "cautious" prior that

rewards only few and small common fragments which have been observed very often, whereas the vast majority of fragments receive a flat prior.

Prior of the Tree Size. The FT we will compute should explain a large number of peaks; We want to favor large trees over small ones. The priors we have introduced so far do exactly the opposite: Many edges result in many probabilities we have to multiply, and small trees are favored over large trees. To this end, we introduce one last prior: We assume $\mathbb{P}(\text{size } |E| \text{ of the tree}) \propto P_{\text{tree-size}}^{|E|}$ where $P_{\text{tree-size}} := P_{\text{tree-norm}} \cdot P_{\text{tree-bonus}}$. Here, $P_{\text{tree-norm}}$ is chosen to counter the effects of the other priors on average, whereas $P_{\text{tree-bonus}}$ is -0.5 by default but can be increased by the user to favor larger trees.

3.2 Likelihood of the Tree

Recall that each considered FT $\mathcal{T} = (V, E)$ is supported by the data $\mathcal{D} = (\mathcal{M}, I)$. This implies the existence of a natural injective mapping $m : V \rightarrow \mathcal{M}$: Each node $v \in V$ is assigned a unique peak $m(v)$ in the fragmentation spectrum. All peaks in the spectrum not assigned to a node of the FT, are noise peaks and also contribute to the likelihood of the tree.

To simplify our computations, we assume independence between the measured peaks in $\mathcal{M} = \{m_1, \dots, m_L\}$, so $\mathbb{P}(\mathcal{D}|\mathcal{T}) = \prod_l \mathbb{P}(m_l|\mathcal{T})$. Here and in the following, m_l refers both to the l -th peak and to its mass. Furthermore, we may assume that for each peak, the probability of the tree to generate some peak depends only on the corresponding hypothetical fragment, so $\mathbb{P}(m(v)|\mathcal{T}) = \mathbb{P}(m(v)|v)$ for all $v \in V$. Then,

$$\mathbb{P}(\mathcal{D}|\mathcal{T}) = \prod_l \mathbb{P}(m_l|\mathcal{T}) = \prod_{v \in V} \mathbb{P}(m(v)|v) \cdot \mathbb{P}(\text{unassigned peaks}|\mathcal{T})$$

for appropriately chosen $\mathbb{P}(m(v)|v)$. Here, $\mathbb{P}(\text{unassigned peaks}|\mathcal{T})$ is the probability that all unassigned peaks $\mathcal{M} - \{m(v) : v \in V\}$, which cannot be explained by \mathcal{T} , are noise peaks. We assume that different noise peaks are again independent.

Unassigned peaks cannot be scored in the FT optimization, as only those nodes and edges are scored that are actually part of the tree. Note again that each node is assigned a unique peak, and that no two nodes are assigned the same peak. We reach

$$\mathbb{P}(\mathcal{D}|\mathcal{T}) = \mathbb{P}(\text{all peaks are noise}) \cdot \prod_{v \in V} \frac{\mathbb{P}(m(v)|v)}{\mathbb{P}(m(v) \text{ is noise})}$$

for appropriate $\mathbb{P}(m(v)|v)$. Again, for fixed data \mathcal{D} , the probability of all peaks being noise simultaneously is a constant, and can be ignored in the optimization of $\mathbb{P}(\mathcal{T}|\mathcal{D})$.

We will now show how to compute the probability of signal peaks and noise peaks. Currently, there exists no general model for the intensity of signal peak in small compound MS. Here, the problem is even harder, as we do not know the fragment’s molecular *structure* but only its molecular formula. Similarly, there exists no sensible model for the mass of noise peaks. To this end, we will use only the peak mass to assess the probability of signal peaks; and only peak intensity to assess the probability of noise peaks. The intensity of peak m is $I(m)$; for brevity we write $I(v) := I(m(v))$.

Probability of Signal Peaks. It has been frequently observed that relative mass deviations are roughly normally-distributed [14, 33]. We found this to be the case for our datasets, too. We assume that the instrument is decently calibrated, then relative mass errors are distributed according to $\mathcal{N}(0, \sigma_m)$. We ignore that no mass errors above some threshold can be observed (truncated normal distribution)

as this has a negligible effect on our computations. The probability to observe a peak with mass $m(v)$ for node/fragment v can be estimated as

$$\mathbb{P}(m(v)|v) = \mathbb{P}\left(|\mathcal{N}(0, \sigma_m)| \geq \frac{|m(v)-\mu(v)|}{\mu(v)}\right) = \operatorname{erf}\left(\frac{|m(v)-\mu(v)|}{\sigma_m\sqrt{2\mu(v)}}\right). \quad (3)$$

This is the two-sided probability that a mass deviation larger than the observed relative mass deviation of peak $m(v)$ will occur by chance. Here, “erf” denotes the error function.

Probability of Noise Peaks. We can estimate the probability that a certain peak is noise, by observing that noise with high intensity are much rarer than noise peaks with small intensity. Previous versions of FT calculation [5,22] implicitly assumed that noise peak intensities are exponentially distributed. For our data, we observe that with increasing intensity, the probability to observe a noise peak of this intensity drops rapidly in the beginning, but stays significantly above zero even for large intensities. This is an example of a long-tailed distribution, and we use the Pareto distribution as a classical example of a long-tailed distribution.

Let x_i be the peak intensity threshold used for peak picking. The probability density function of the Pareto distribution is $\alpha_i x_i^{\alpha_i} / x^{\alpha_i+1}$ for mass x . α_i is the shape parameter of the distribution and can be learned from data using a maximum likelihood estimator. The probability of observing a noise peak m with intensity I or higher, is $\mathbb{P}(m \text{ is noise}) = \alpha_i x_i^{\alpha_i} / I^{\alpha_i+1}$.

3.3 Posterior Probability of the Tree

From the above we infer that

$$\mathbb{P}(T) \cdot \mathbb{P}(\mathcal{T}|\mathcal{D}) \propto P_{\text{root}}(r) \cdot \prod_{e \in E} (P_{\text{edge}}(e) \cdot P_{\text{tree-size}}) \cdot \prod_{v \in V} \left(\operatorname{erf}\left(\frac{|m(v)-\mu(v)|}{\sigma_m\sqrt{2\mu(v)}}\right) \Big/ \frac{\alpha_i x_i^{\alpha_i}}{I(v)^{\alpha_i+1}} \right) \quad (4)$$

for FT $\mathcal{T} = (V, E)$ with root $r \in V$. This allows us to weight the edges of the fragmentation graph: For each edge (u, v) we set its edge weight

$$w(u, v) := \log P_{\text{edge}}(u, v) + \log P_{\text{tree-size}} + \log \operatorname{erf}\left(\frac{|m(v)-\mu(v)|}{\sigma_m\sqrt{2\mu(v)}}\right) - \log \frac{\alpha_i x_i^{\alpha_i}}{I(v)^{\alpha_i+1}}. \quad (5)$$

With these edge weights, the colorful subtree of maximum weight corresponds to the FT with maximum posterior probability; more precisely, ordering colorful subtrees with respect to their weight, is equivalent to ordering the corresponding FTs by posterior probability.

3.4 Hypothesis-driven Recalibration.

To improve the quality of FTs, we have implemented a hypothesis-driven recalibration [4]. We are given one fragmentation spectrum at a time. For each candidate molecular formula explaining the root, we compute a FT, and then use the theoretical masses of all nodes in the FT as references to recalibrate the sample spectrum. We then compute the optimal FT for the recalibrated sample spectrum and the candidate molecular formula, and use this score to evaluate which root molecular formula best explains the data. Then, the recalibration is *discarded*, returning to the original measured sample spectrum, and the next root molecular formula is processed.

We note that our hypothesis-driven recalibration (HDR) is fundamentally different from, say, the recalibration proposed in [28]: Using HDR, each spectrum is recalibrated individually, using each peaks best theoretical explanation as anchors for the mass correction. In this way, we do not require a homogeneous dataset of mass spectra to start the recalibration process.

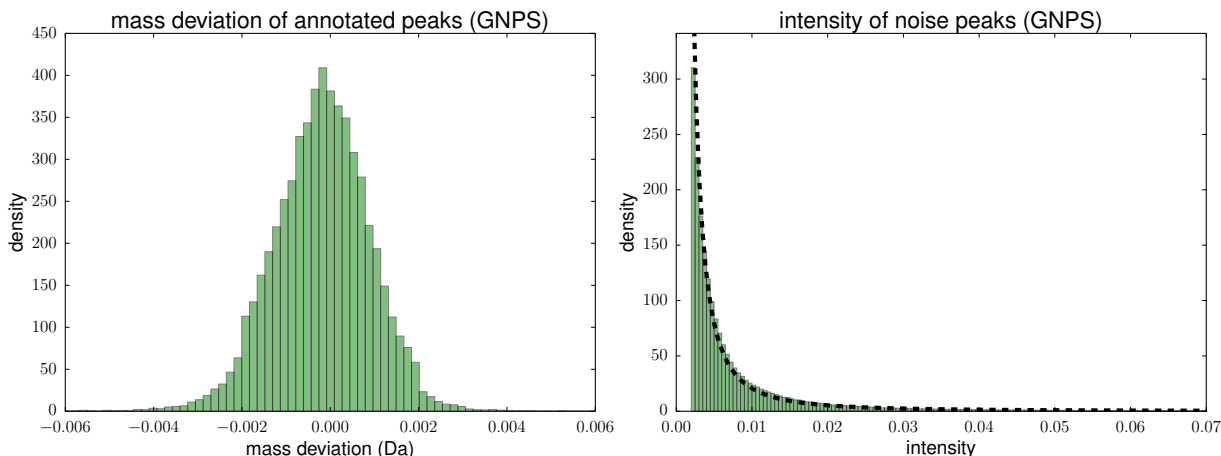


Fig. 2. Left: Normalized histogram of the mass error distribution. Right: Normalized histogram of the noise peak intensity distribution and fitted Pareto distribution (dashed line). GNPS dataset.

4 Results

Datasets. The GNPS dataset was downloaded from the GNPS database in December 2014 (<http://gnps.ucsd.edu>). We analyze a total of 2006 non-peptide compounds with mass below 1010 Da where mass spectra were recorded in positive mode, and mass accuracy of the parent mass was below 10 ppm. For each compound, a single fragmentation spectra was recorded on an Agilent QTOF with electrospray ionization. The *Agilent* dataset is available under the name “MassHunter Forensics/Toxicology PCDL” (version B.04.01) from Agilent Technologies (Santa Clara, CA, USA). The commercial library has been cleaned by idealizing peak masses and removing noise peaks, but Agilent provided us with an uncorrected version of this dataset, which is used here. For this dataset, 2120 compounds fulfill the above criteria. Fragmentation spectra at collision energies 10, 20, and 40 eV were recorded on an Agilent 6500 Series QTOF system with electrospray ionization. Only relative intensities were recorded, so preprocessing was applied to merge spectra recorded at different collision energies. The masses of the compounds in both dataset range from 85 Da to 980 Da with an average mass of 340 Da.

Each dataset was split into two disjoint batches: The **CHNOPS** batch contains compounds that use solely elements CHNOPS (GNPS: 1589 compounds, Agilent: 1540 compounds), whereas compounds from the **contains FCIBrI** batch contain at least one atom from FCIBrI (GNPS: 417, Agilent: 580).

Estimating the (Hyper)parameters. To apply our model to real data, we have to fit the (hyper)parameters for priors and the likelihood estimation. We optimize hyperparameters in an iterative procedure, using FTs from the previous round to determine parameters of the current. See the long version of this paper for all details.

For both datasets, we observe that mass errors follow a normal distribution, see Fig. 2. By manual inspection, we estimate $MA = 10$ ppm. The maximum likelihood estimation for our datasets leads to a normal distribution with $\sigma_m = 5.5$. But we find that using a higher standard deviation $\sigma_m = 10$ gives us better results due to the lower weight our scoring is giving to the mass deviation. In both datasets, we observe an exponential decay of noise peaks (i.e. peaks without an explanation for the parent molecular formula) with increasing intensity, see Fig. 2. We estimate $x_i = 0.002$ and $\alpha_i = 0.34$ for GNPS and $x_i = 0.005$, and $\alpha_i = 0.5$ for Agilent.

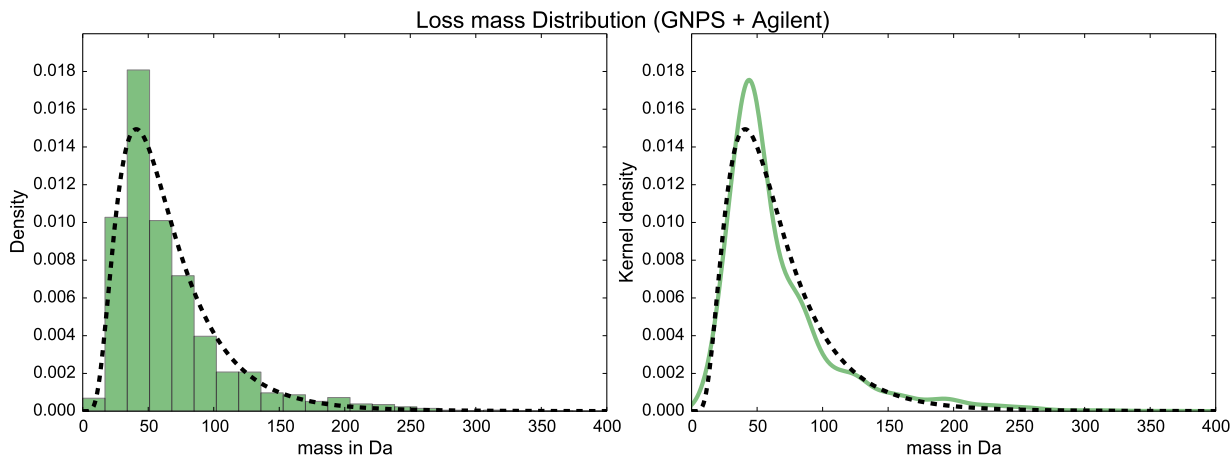


Fig. 3. Loss mass distribution, after the final round of parameter estimation. Frequencies of the losses are weighted by the intensity of their peaks. The frequency of the identified common losses have been decreased to the value of the log-normal distribution. Left: Normalized histogram for bin width 17 Da. Right: Kernel density estimation. Black (dashed): Maximum likelihood estimate of the log-normal distribution.

Common losses are outliers, in the sense that their frequency is far higher than we would expect for a loss of this mass. During our iterative procedure we find 34 common losses, 13 of them were already listed in [5, 21, 22], further 16 losses could be assigned to known structures. See Fig. 3 for the agreement between the observed distribution of loss masses (corrected for common losses) and the fitted log-normal distribution. We estimate $\mu_{ls} = 4.02$ and $\sigma_{ls} = 0.31$ for the loss mass distribution, with mode $e^{\mu_{ls}} = 55.84$ Da.

Evaluation Results. There is practically no way to determine the *ground truth* of the fragmentation process; even the comparison with fragmentation cascades obtained using MS^n data is not a satisfactory solution. Manual evaluation is very work-intensive and, hence, infeasible for the two large-scale datasets considered here. To this end, we evaluate the performance of our method in answering a question where the true answer is known.

To identify the *molecular formula* of a compound, we rank the FTs and, hence, the molecular formulas according to the reached posterior probabilities. Besides mass accuracy and noise peak intensity, the user has to provide the alphabet of elements the unknown compound can be made from. For batch CHNOPS we use this alphabet of elements without further restrictions. For batch “contains FCIBrI” we assume that we know upfront which of the elements, besides CHNOPS, *may* be contained in the compound. Such information can be obtained from the isotope pattern and the tandem mass spectrum using, say, machine learning (manuscript in preparation).

See Fig. 4 for the molecular formula prediction performance of the method. As expected, prediction is much harder for the batch containing halogens. Also, the new scoring significantly increases the number of instances where we can recover the correct molecular formula. We evaluate our method both against the method from [21, 22] as published there, using a dynamic programming (DP) approach for finding the best FT; plus, scores from [21, 22] together with the ILP from [23].

As our second evaluation of FT quality, we want to search a spectral library with a query compound *not* contained in the database; the goal of this search is to find compounds that are structurally similar [7, 21]. In a leave-one-out evaluation, we use each compound as our query; for each query, we sort all remaining entries of the database with respect to our similarity score, then evaluate the average chemical similarity of the first k entries. Instead of forcing each query

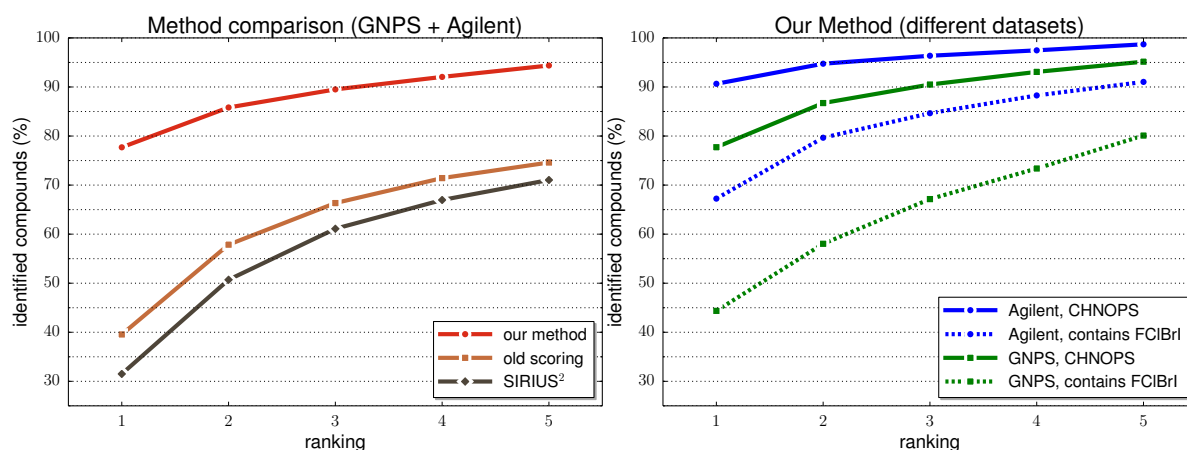


Fig. 4. Performance evaluation, percentage of instances (y-axis) where the correct molecular formula is present in the TOP k for $k = 1, \dots, 5$ (x-axis). Left: Performance evaluation for different methods on both datasets. Methods are “our method” (the method presented here), “old scoring” (scores from [21,22] with ILP), “SIRIUS²” (scores from [21,22] with DP). Right: Performance for the two compound batches (CHNOPS as solid line, “contains FCIBrI” as dashed line) and the two datasets (GNPS green, Agilent blue).

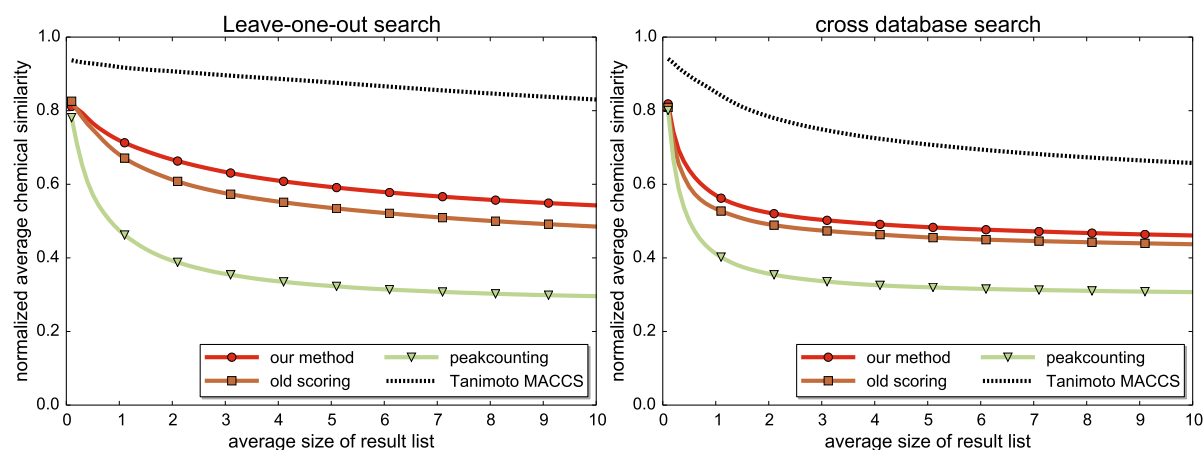


Fig. 5. Similarity search performance plots for chemical similarity. Methods “our method” and “old scoring” compute FTs using ILP and compare trees via tree alignments [21]. Method “peak counting” uses direct spectral comparison. Method “MACCS” uses fingerprints computed from the structure of the compound. Left: Similarity search with Leave-one-out strategy on both datasets. Right: Similarity search across the databases. Compounds from GNPS are searched in Agilent and vice-versa.

compound to return the same number of entries, we just enforce that in average each query returns k entries. The cross database evaluation is done analogously, but using GNPS compounds as query and searching in the Agilent database (and vice-versa).

We measure chemical similarity using Tanimoto coefficients and PubChem fingerprints. See Fig. 5 for a comparison of the old and new FTs, using tree alignments from [21] to compute similarity scores. We also compare to direct spectral comparison via peak counting, which gave us best results of all methods for direct spectral comparison on these datasets, and Tanimoto scores computed by MACCS fingerprint. Remark that for computing MACCS fingerprints, the structure of the compound have to be known, while for spectral and FT alignments only the spectrum is necessary. We normalize score such that the optimal method reaches similarity score 1, and the random method reaches 0.

5 Conclusion

We have presented a maximum a posteriori estimator for the problem of computing fragmentation trees, that performs significantly better than previous approaches for the problem. Identification performance can be significantly improved by adding isotope pattern information [3, 8, 22] but this data is not available for the two datasets. The only alternative method for estimating a molecular formula (solely) from tandem MS data is the commercial MOLGEN-MS/MS software [17, 25], which performs roughly on par with SIRIUS² (DP version) [28].

We used the new scoring in the CASMI (Critical Assessment of Small Molecule Identification) challenge 2013 to determine the molecular formula of 12 unknown compounds. Using the fragmentation tree analysis as presented here, we correctly identified 8 molecular formulas, and placed an additional 3 in the TOP2 [8]. In conjunction with isotope pattern analysis [3] we identified 10 out of 12 molecular formulas, and our method SIRIUS was selected “best automated tool” of the molecular formula challenge [18]. Furthermore, the new scoring was used to compute fragmentation trees as part of a novel approach for determining molecular fingerprints from tandem MS data which, in turn, can be used to search molecular structure databases [27]. Here, the improved FT structure resulted in significantly improved prediction performance.

Acknowledgments. We thank Frank Kuhlmann and Agilent Technologies, Inc. (Santa Clara, USA) for providing uncorrected peak lists of their spectral library. We thank Pieter Dorrestein, Nuno Bandeira (University of California) and the GNPS community for making their data accessible.

References

1. F. Allen, R. Greiner, and D. Wishart. Competitive fragmentation modeling of ESI-MS/MS spectra for putative metabolite identification. *Metabolomics*, 2014. Doi 10.1007/s11306-014-0676-4.
2. M. Baker. Metabolomics: From small molecules to big ideas. *Nat Methods*, 8:117–121, 2011.
3. S. Böcker, M. Letzel, Zs. Lipták, and A. Pervukhin. SIRIUS: Decomposing isotope patterns for metabolite identification. *Bioinformatics*, 25(2):218–224, 2009.
4. S. Böcker and V. Mäkinen. Combinatorial approaches for mass spectra recalibration. *IEEE/ACM Trans Comput Biol Bioinform*, 5(1):91–100, 2008.
5. S. Böcker and F. Rasche. Towards de novo identification of metabolites by analyzing tandem mass spectra. *Bioinformatics*, 24:I49–I55, 2008. Proc. of *European Conference on Computational Biology (ECCB 2008)*.
6. M. A. Cooper and D. Shlaes. Fix the antibiotics pipeline. *Nature*, 472(7341):32, 2011.
7. W. Demuth, M. Karlovits, and K. Varmuza. Spectral similarity versus structural similarity: Mass spectrometry. *Anal Chim Acta*, 516(1-2):75–85, 2004.
8. K. Dührkop, F. Hufsky, and S. Böcker. Molecular formula identification using isotope pattern analysis and calculation of fragmentation trees. *Mass Spectrom*, 3(special issue 2):S0037, 2014.
9. M. Gerlich and S. Neumann. MetFusion: integration of compound identification strategies. *J Mass Spectrom*, 48(3):291–298, 2013.
10. M. Heinonen, H. Shen, N. Zamboni, and J. Rousu. Metabolite identification and molecular fingerprint prediction via machine learning. *Bioinformatics*, 28(18):2333–2341, 2012. Proc. of *European Conference on Computational Biology (ECCB 2012)*.
11. H. Horai, M. Arita, S. Kanaya, Y. Nihei, T. Ikeda, K. Suwa, Y. Ojima, K. Tanaka, S. Tanaka, K. Aoshima, Y. Oda, Y. Kakazu, M. Kusano, T. Tohge, F. Matsuda, Y. Sawada, M. Y. Hirai, H. Nakanishi, K. Ikeda, N. Akimoto, T. Maoka, H. Takahashi, T. Ara, N. Sakurai, H. Suzuki, D. Shibata, S. Neumann, T. Iida, K. Tanaka, K. Funatsu, F. Matsuura, T. Soga, R. Taguchi, K. Saito, and T. Nishioka. MassBank: A public repository for sharing mass spectral data for life sciences. *J Mass Spectrom*, 45(7):703–714, 2010.
12. F. Hufsky, K. Scheubert, and S. Böcker. Computational mass spectrometry for small molecule fragmentation. *Trends Anal Chem*, 53:41–48, 2014.
13. F. Hufsky, K. Scheubert, and S. Böcker. New kids on the block: Novel informatics methods for natural product discovery. *Nat Prod Rep*, 31(6):807–817, 2014.
14. N. Jaitly, M. E. Monroe, V. A. Petyuk, T. R. W. Clauss, J. N. Adkins, and R. D. Smith. Robust algorithm for alignment of liquid chromatography-mass spectrometry analyses in an accurate mass and time tag data analysis pipeline. *Anal Chem*, 78(21):7397–7409, 2006.

15. T. Kind and O. Fiehn. Seven golden rules for heuristic filtering of molecular formulas obtained by accurate mass spectrometry. *BMC Bioinformatics*, 8:105, 2007.
16. L. C. Menikarachchi, S. Cawley, D. W. Hill, L. M. Hall, L. Hall, S. Lai, J. Wilder, and D. F. Grant. MolFind: A software package enabling HPLC/MS-based identification of unknown chemical structures. *Anal Chem*, 84(21):9388–9394, 2012.
17. M. Meringer, S. Reinker, J. Zhang, and A. Müller. MS/MS data improves automated determination of molecular formulas by mass spectrometry. *MATCH-Commun Math Co*, 65:259–290, 2011.
18. T. Nishioka, T. Kasama, T. Kinumi, H. Makabe, F. Matsuda, D. Miura, M. Miyashita, T. Nakamura, K. Tanaka, and A. Yamamoto. Winners of CASMI2013: Automated tools and challenge data. *Mass Spectrom*, 3(special issue 2):S0039, 2014.
19. G. J. Patti, O. Yanes, and G. Siuzdak. Metabolomics: The apogee of the omics trilogy. *Nat Rev Mol Cell Biol*, 13(4):263–269, 2012.
20. T. Pluskal, T. Uehara, and M. Yanagida. Highly accurate chemical formula prediction tool utilizing high-resolution mass spectra, MS/MS fragmentation, heuristic rules, and isotope pattern matching. *Anal Chem*, 84(10):4396–4403, 2012.
21. F. Rasche, K. Scheubert, F. Hufsky, T. Zichner, M. Kai, A. Svatoš, and S. Böcker. Identifying the unknowns by aligning fragmentation trees. *Anal Chem*, 84(7):3417–3426, 2012.
22. F. Rasche, A. Svatoš, R. K. Maddula, C. Böttcher, and S. Böcker. Computing fragmentation trees from tandem mass spectrometry data. *Anal Chem*, 83(4):1243–1251, 2011.
23. I. Rauf, F. Rasche, F. Nicolas, and S. Böcker. Finding maximum colorful subtrees in practice. *J Comput Biol*, 20(4):1–11, 2013.
24. M. Rojas-Chertó, P. T. Kasper, E. L. Willighagen, R. J. Vreeken, T. Hankemeier, and T. H. Reijmers. Elemental composition determination based on MSⁿ. *Bioinformatics*, 27:2376–2383, 2011.
25. K. Scheubert, F. Hufsky, and S. Böcker. Computational mass spectrometry for small molecules. *J Cheminform*, 5:12, 2013.
26. J. Senior. Partitions and their representative graphs. *Amer J Math*, 73(3):663–689, 1951.
27. H. Shen, K. Dührkop, S. Böcker, and J. Rousu. Metabolite identification through multiple kernel learning on fragmentation trees. *Bioinformatics*, 30(12):i157–i164, 2014. Proc. of *Intelligent Systems for Molecular Biology (ISMB 2014)*.
28. M. A. Stravs, E. L. Schymanski, H. P. Singer, and J. Hollender. Automatic recalibration and processing of tandem mass spectra using formula annotation. *J Mass Spectrom*, 48(1):89–99, 2013.
29. M. N. Thaker, W. Wang, P. Spanogiannopoulos, N. Waglechner, A. M. King, R. Medina, and G. D. Wright. Identifying producers of antibacterial compounds by screening for antibiotic resistance. *Nat Biotechnol*, 31(10):922–927, 2013.
30. D. S. Wishart, C. Knox, A. C. Guo, R. Eisner, N. Young, B. Gautam, D. D. Hau, N. Psychogios, E. Dong, S. Bouatra, R. Mandal, I. Sinelnikov, J. Xia, L. Jia, J. A. Cruz, E. Lim, C. A. Sobsey, S. Shrivastava, P. Huang, P. Liu, L. Fang, J. Peng, R. Fradette, D. Cheng, D. Tzur, M. Clements, A. Lewis, A. D. Souza, A. Zuniga, M. Dawe, Y. Xiong, D. Clive, R. Greiner, A. Nazyrova, R. Shaykhtudinov, L. Li, H. J. Vogel, and I. Forsythe. HMDB: A knowledgebase for the human metabolome. *Nucleic Acids Res*, 37:D603–D610, 2009.
31. S. Wolf, S. Schmidt, M. Müller-Hannemann, and S. Neumann. In silico fragmentation for computer assisted identification of metabolite mass spectra. *BMC Bioinformatics*, 11:148, 2010.
32. O. Yanes, J. Clark, D. M. Wong, G. J. Patti, A. Sánchez-Ruiz, H. P. Benton, S. A. Trauger, C. Despons, S. Ding, and G. Siuzdak. Metabolic oxidation regulates embryonic stem cell differentiation. *Nat Chem Biol*, 6(6):411–417, 2010.
33. R. Zubarev and M. Mann. On the proper use of mass accuracy in proteomics. *Mol Cell Proteomics*, 6(3):377–381, 2007.